

This article was downloaded by: [UNSA]

On: 02 April 2013, At: 09:11

Publisher: Taylor & Francis

Informa Ltd Registered in England and Wales Registered Number: 1072954 Registered office: Mortimer House, 37-41 Mortimer Street, London W1T 3JH, UK



International Journal of Systems Science

Publication details, including instructions for authors and subscription information:
<http://www.tandfonline.com/loi/tsys20>

Collaborative multi-target tracking in wireless sensor networks

Jing Teng^a, Hichem Snoussi^b & Cédric Richard^c

^a School of Control and Computer Engineering, North China Electric Power University, Beijing 102206, China

^b ICD/LM2S, University of Technology of Troyes, Troyes 10000, France

^c Fizeau Laboratory (UNS, CNRS UMR 6525, Observatoire de la Côte d'Azur), University of Nice Sophia-Antipolis, 06108 Nice cedex 02, France

Version of record first published: 20 May 2011.

To cite this article: Jing Teng, Hichem Snoussi & Cédric Richard (2011): Collaborative multi-target tracking in wireless sensor networks, International Journal of Systems Science, 42:9, 1427-1443

To link to this article: <http://dx.doi.org/10.1080/00207721.2011.581398>

PLEASE SCROLL DOWN FOR ARTICLE

Full terms and conditions of use: <http://www.tandfonline.com/page/terms-and-conditions>

This article may be used for research, teaching, and private study purposes. Any substantial or systematic reproduction, redistribution, reselling, loan, sub-licensing, systematic supply, or distribution in any form to anyone is expressly forbidden.

The publisher does not give any warranty express or implied or make any representation that the contents will be complete or accurate or up to date. The accuracy of any instructions, formulae, and drug doses should be independently verified with primary sources. The publisher shall not be liable for any loss, actions, claims, proceedings, demand, or costs or damages whatsoever or howsoever caused arising directly or indirectly in connection with or arising out of the use of this material.

Collaborative multi-target tracking in wireless sensor networks

Jing Teng^{a*}, Hichem Snoussi^b and Cédric Richard^c

^aSchool of Control and Computer Engineering, North China Electric Power University, Beijing 102206, China;
^bICD/LM2S, University of Troyes, Troyes 10000, France; ^cFizeau Laboratory (UNS, CNRS UMR 6525, Observatoire de la Côte d'Azur), University of Nice Sophia-Antipolis, 06108 Nice cedex 02, France

(Received 31 August 2010; final version received 13 February 2011)

A collaborative variational/Monte Carlo scheme is proposed to solve the multi-target tracking (MTT) problem in wireless sensor networks (WSNs). The prime motivation of our work is to balance the inherent trade-off between the resource consumption and the accuracy of the target tracking. For the sake of resource efficiency, we reduce the MTT problem to distributed cluster-based variational target tracking when the targets are far apart; and switch to data association only when the targets are gathered, leading to ambiguous measurements. The sequential Monte Carlo (SMC) method is employed to assign the ambiguous measurements to specific targets or clutter based on association probabilities. The associated observations are then incorporated by the variational filter, where the distribution of involved particles is approximated by a simple Gaussian distribution for each target. In addition, considering the situation that the number of targets is varying, an hypothesis test is integrated into the collaborative scheme, to deal with the cases of arrivals of new targets and disappearances of the tracked targets. The effectiveness of the proposed scheme is evaluated and compared with the classic SMC MTT algorithm in terms of tracking accuracy, computation complexity and energy consumption.

Keywords: multi-target tracking; variational filtering; sequential Monte Carlo; data association; wireless sensor network

1. Introduction

Multi-target tracking (MTT) deals with the state estimation of several moving targets. It is not a trivial extension of single target tracking but rather a challenging topic of research (Khan, Balch, and Dellaert 2006). Due to the fact that in most practical tracking applications the sensors yield unlabeled measurements of the targets (Vermaak, Godsill, and Pérez 2005), the main difficulty of MTT comes from the assignment of a given measurement to a specific target (Kreucher, Kastella, and Hero 2005), which always requires exhaustive testing of all possibilities leading to great resource consumption. Furthermore, clutter measurements may arise due to multi-path effects, sensor errors, spurious objects, etc., further increasing the complexity of the data association problem. Therefore, existing MTT algorithms generally present two basic ingredients: an estimation algorithm coupled with a data association method (Hue, Le Cadre, and Pérez 2006). In fact, MTT is much easier when the targets are distinctive and do not interact with each other. It can be solved by employing multiple independent trackers. However, for those targets that are similar in appearance, obtaining their correct trajectories becomes significantly more challenging when they are in close

proximity or present partial occlusions (Song, Cui, Zha, and Zhao 2008). Therefore, much of the theory of MTT was developed for centralised processing (Liu, Chu, and Reich 2007). Whereas wireless sensor networks (WSNs) demand a somewhat different approach, which focus on scalable performance and management of limited resources. In WSNs, the main challenge to implement an MTT algorithm is to reduce the computational complexity of the problem while still providing reasonable tracking performance. This challenging problem has attracted considerable attention in the literature (Yang and Sikdar 2003; He and Hou 2005; Liu et al. 2007).

Data association has been the primary focus of the MTT literature (Liu et al. 2007). Traditionally, the nearest neighbour (NN) approach, which utilises the closest measurement to the predicted target measurement, is the simplest approach for MTT (Blackman and Popoli 1999; Hue, Le Cadre, and Pérez 2002b; Song, Lee, and Ryu 2005). The NN filter assumes at any time that the NN measurement is target-originated and a standard Kalman filter (KF) is then used to update the target state estimate. However, the NN measurements may be originated from a clutter, leading to filter divergence in many situations.

*Corresponding author. Email: jing.teng@ncepu.edu.cn

Performance of the NN filter has been deeply analysed in Li and Bar-Shalom (1996). As long as the data association is considered in a deterministic way, all possible associations must be exhaustively enumerated (Hue et al. 2002b). Multiple hypothesis tracking (MHT) was proposed by Reid (1979). The idea is to recursively enumerate the set of all possible associations (called hypotheses) of measurements to existing tracks, new tracks and false alarms (namely clutters) while respecting the mutual exclusion association constraint. An advantage of this approach is that the number of tracks is not required to be known *a priori* because track initiations and terminations are explicitly hypothesised. Furthermore, data association decisions are effectively delayed until more data are received since multiple hypotheses are kept. Therefore, MHT can address low detection probability, high false alarm rates, initiation and termination of tracks, and delayed measurements. However, this approach suffers from large storage space requirements and exponentially increasing processing. This leads to an NP-hard problem because the number of possible associations increases exponentially with time. To cope with this problem, pruning and gating have been proposed to eliminate the unlikely hypotheses. However, good hypotheses may be eliminated as well. The joint probabilistic data association filter (JPDAF) proposed by Fortmann, Bar-Shalom, and Scheffe (1980), consisting of updating each individual track state with weighted combinations of all measurements, is an alternative solution. This approach is based on computing the probability that measurements can be associated with tracks with respect to the mutual exclusion constraint. A disadvantage of this approach is that the number of targets needs to be known *a priori*. In fact, JPDAF is a particular way of combining the multiple hypotheses generated by MHT into a single hypothesis and, therefore, can be viewed as an instance of MHT. Sequential Monte Carlo (SMC) methods are a class of algorithms which sample from complex probability distributions conditioned on observations. The application of SMC-based approach to data association (SMCDA) has been proposed in Hue, Le Cadre, and Pérez (2002a) and Oh, Russell, and Sastry (2004), where samples are drawn according to the association probabilities. The sample with the highest probability is considered as the best association hypothesis. As the hypotheses are not explicitly enumerated in SMCDA, the large storage space is no longer required compared to MHT. Besides, the SMCDA approach is very easy to implement and can be applied under very general hypotheses to cope with heavy clutters situations.

The data association approaches mentioned above consider all possible events related to data association, which makes MTT an expensive task in terms of

sensing, computation and communication. Concerning the extremely stringent resource in WSNs, an energy-aware distributed signal processing scheme is proposed in this article. The idea is to reduce the MTT problem to single target tracking when targets are far apart and switch to MTT only when data association becomes ambiguous. As targets can travel arbitrarily and no *a priori* information on targets motion is provided, a general state evolution model is proposed to describe the hidden states. For energy efficiency, each target is tracked by a cluster of sensors using a Variational Filter (VF; Teng, Snoussi, and Richard 2007a, b; Teng, Snoussi, Richard, and Zhou 2009). By adopting the VF method, the inter-cluster information exchange for one target is reduced to one single Gaussian statistic, dramatically cutting down the resource consumption of the whole network. Since the measurement incorporation and the approximation of the filtering distribution are jointly performed by variational calculus, an effective and lossless compression is achieved compared to the classical particle filtering and other approximation method. With respect to the clustering rule, we simply assume that the sensors which have detected the appearance of a same target form a cluster. Once the targets move closer, their clusters collide. Collision is flagged when ambiguous observation data are generated, which means that a sensor can detect several targets at a time. To cope with this situation, the tracking switches to MTT mode, and the activated clusters merge into one cluster. The new leader is elected based on the residual energy comparison among the original activated cluster heads (CHs). The SMCDA method is employed to assign the ambiguous observations to specific targets or the clutter based on the association probabilities. The variational tracking is delayed after the SMCDA phase to incorporate the rest of observations. Owing to the implicit compression of VF, the temporal dependence of each target is reduced to a Gaussian distribution, which dramatically cuts off the inter-cluster communication during hand-off operations.

The rest of this article is organised as follows. In Section 2, we provide a brief problem statement and make some assumptions for MTT, in order to give an overview of the proposed collaborative MTT scheme. The VF algorithm for MTT is formulated in Section 3, with a detailed description in Section 4. Section 5 is dedicated to the probabilistic data association phase, which is invoked once ambiguous data are observed. By cluster merging, ambiguous data are collected and then associated with specific targets or clutter by the SMCDA method. Section 6 describes the hypothesis test method used in case of arrival of new target and/or disappearance of already tracked targets. Performance of the proposed scheme is studied by simulations

in Section 7. Finally, we conclude and suggest future directions for research in Section 8.

2. Problem statement and overview

We assume the following properties of the WSN for MTT:

- All the sensors are stationary and location-aware.
- Sensors are randomly and uniformly deployed with density ρ_s . Their sensing ranges are identically set to r_s , and similarly, the radio communication ranges r_c are identical too. In cluster-based target tracking, the CHs are responsible for updating the target beliefs by the VF algorithm with observations collected from their slaves. To ensure that each sensor in the WSN is capable of performing the task of an active CH, all of them are assumed to have an identical configuration with sufficient battery and computational power. Each of the sensors keeps an address list of its neighbouring sensor IDs and locations by exchanging information between each other. Furthermore, all the sensors in the network are synchronised for efficient data communication.

Concerning the coverage problem, the deployment of sensors must ensure a high probability of detecting the appearance of a target. During the tracking phase, at least three sensors are required to simultaneously detect the target and to report their observations, in order to generate enough information for further processing. According to the network properties described above, the distribution of the sensors in any given area A is Poisson with the rate $\rho_s A$. Therefore, the probability for any arbitrary point in the field to be sensed by at least three sensors is $p_s = \sum_{i=3}^{\infty} \frac{e^{-\rho_s \pi r_s^2} (\rho_s \pi r_s^2)^i}{i!}$ (Yang and Sikdar 2003). Substituting a desirable value for p_s , (e.g. $p_s = 0.99$), the optimal node density ρ_s and sensing range r_s can be easily inferred.

At the initialisation step, all of the sensors are set to the ‘Sensing’ mode to monitor the whole region. As soon as an intrusion is detected, sensors within the phenomenon of interest exchange information to form a cluster dynamically. CH_0 is randomly chosen among these sensors since their residual energy are identical initially. The other sensors in the activated cluster consequently become the slave sensors, which communicate with the CH directly and report their observations. As the target travels through the sensing field, the energy-intensive task of CH_t is assigned to the

sensor with the most residual energy in the activated cluster, to balance energy consumption. The size of an activated cluster is determined by the relationship between the communication range r_c and the sensing range r_s (Chen, Hou, and Sha 2004). In order to ensure tracking accuracy and energy efficiency, the communication range is assumed to be twice the sensing range, namely $r_c = 2r_s$. Therefore, with respect to a single target, only one cluster is formed, and the intra-cluster communication is restricted to one-hop. In fact, it is possible that several intrusions are detected at the same time. If the intrusions are far apart, namely each sensor in one cluster only gets one measurement related to the well identified target, we assume that the cluster is tracking a single target. Single target tracking algorithms are parallelly performed in different CHs. Otherwise, ambiguous measurements are observed, which could be generated by either the clutter or by the other targets. The configuration of the sensor network guarantees that the distances between the sensors detecting a same target are smaller than r_c , which means that they could communicate with each other in one-hop. It is thus reasonable to assume that the CH with data association ambiguity only needs to communicate with its neighbouring CHs to collect a complete set of ambiguous measurements. If the number of ambiguous measurements N_{amb} is smaller than three and the rest of the observations are greater than three, we simply discard the ambiguous observations and use the rest of the observations to track the targets. Otherwise, the CH with the most residual energy among the neighbouring CHs with data association ambiguity is elected to be the new leader. The data association phases is performed on the set of ambiguous observations by the new leader using the SMCDA method proposed in Hue et al. (2002a). Instead of propagating a large number of particles, the particles for data association are only generated when necessary and are sampled from the Gaussian distributions kept by the VF single target tracking algorithms performed in the original CHs. In fact, the SMCDA associates and incorporates the ambiguous measurements at the same time. The particles generated by the SMCDA phase are separated for each target and are directly employed to incorporate the rest of observations in respective CHs. After the run of the VF algorithm, estimates of the targets locations are refined. Especially, the distributions of the particles are naturally approximated by a simple Gaussian distribution for each target. To sum up, the MTT problem is tackled by a collaborative scheme, where each target is tracked by a VF, and the SMCDA phase is invoked only when ambiguous measurements are collected. An overview of the collaborative MTT scheme is illustrated by Figure 1.

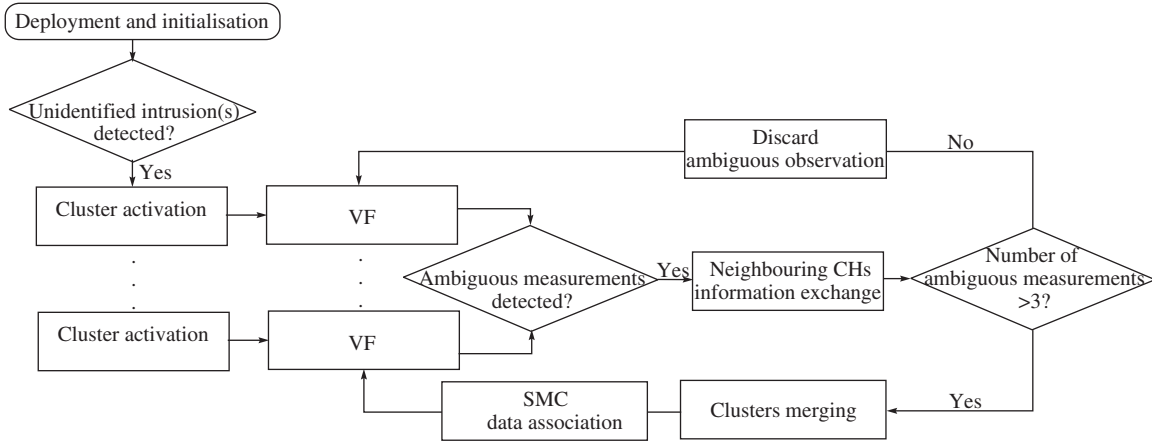


Figure 1. Block diagram of the collaborative MTT scheme.

3. Problem formulation for VF

The VF algorithm for target tracking inherits many desirable properties from the Bayesian Inference framework. An important step in Bayesian multi-target tracking is the recursive estimation of the predictive distribution as follows,

$$p(\mathbf{X}_t | \mathbf{Z}_{1:t-1}) = \int p(\mathbf{X}_t | \mathbf{X}_{t-1}) p(\mathbf{X}_{t-1} | \mathbf{Z}_{1:t-1}) d\mathbf{X}_{t-1},$$

where $\mathbf{X}_t = \{\mathbf{x}_t^j\}_{j=1}^M$,

$$\text{and } \mathbf{x}_t^j \in \mathbb{R}^{n_x}, \quad \forall j = 1, \dots, M,$$

M is the number of targets .

The conditional distribution $p(\mathbf{X}_t | \mathbf{X}_{t-1})$ is employed to model the prior time evolution of the target state. By incorporating the observation model $p(\mathbf{Z}_t | \mathbf{X}_t)$, the new estimate of the targets state \mathbf{X}_t is updated based on the predictive distribution $p(\mathbf{X}_t | \mathbf{Z}_{1:t-1})$:

$$p(\mathbf{X}_t | \mathbf{Z}_{1:t}) = \frac{p(\mathbf{Z}_t | \mathbf{X}_t) p(\mathbf{X}_t | \mathbf{Z}_{1:t-1})}{p(\mathbf{Z}_t | \mathbf{Z}_{1:t-1})},$$

where $p(\mathbf{Z}_t | \mathbf{Z}_{1:t-1}) = \int p(\mathbf{Z}_t | \mathbf{X}_t) p(\mathbf{X}_t | \mathbf{Z}_{1:t-1}) d\mathbf{X}_t$.

The observation model $p(\mathbf{Z}_t | \mathbf{X}_t)$ depends on the sensing mode employed by the sensors, while the state evolution model $p(\mathbf{X}_t | \mathbf{X}_{t-1})$ is always described by a parametric model. We describe these two models in the following sections.

3.1. General state evolution model

The targets to be tracked are modelled by independent Markovian dynamics. Let M be the number of targets, $\mathbf{X}_t = \{\mathbf{x}_t^j\}_{j=1}^M$ denotes the targets temporal positions, where each component \mathbf{x}_t^j is assumed to evolve

according to a general state evolution model. This model is more appropriate to the practical non-linear and non-Gaussian situations, where no *a priori* information on the target velocity or its acceleration is available. The target position $\mathbf{x}_t^j \in \mathbb{R}^{n_x}$ at instant t is assumed to follow a Gaussian model, where its expectation $\boldsymbol{\mu}_t^j$ and the precision matrix $\boldsymbol{\lambda}_t^j$ are both random. The randomness is used here to further capture the uncertainty of the state distribution, which leads to a probability distribution covering a wide range of tail behaviours, allowing discrete jumps in the target trajectory. A practical choice of these distributions is a Gaussian distribution for the expectation $\boldsymbol{\mu}_t^j$ and a n_x -dimensional Wishart distribution for the precision matrix $\boldsymbol{\lambda}_t^j$. In an other word, the hidden state \mathbf{x}_t^j is extended to an augmented state $\boldsymbol{\alpha}_t^j = (\mathbf{x}_t^j, \boldsymbol{\mu}_t^j, \boldsymbol{\lambda}_t^j)$, yielding a hierarchical model as follows,

$$\begin{cases} \mathbf{x}_t^j \sim \mathcal{N}(\mathbf{x}_t^j | \boldsymbol{\mu}_t^j, \boldsymbol{\lambda}_t^j) \\ \boldsymbol{\mu}_t^j \sim \mathcal{N}(\boldsymbol{\mu}_t^j | \boldsymbol{\mu}_{t-1}^j, \bar{\boldsymbol{\lambda}}^j), \quad \forall j = 1, \dots, M, \\ \boldsymbol{\lambda}_t^j \sim \mathcal{W}_{n_x}(\boldsymbol{\lambda}_t^j | \bar{\mathbf{V}}^j, \bar{n}^j) \end{cases} \quad (3)$$

where $\bar{\boldsymbol{\lambda}}^j$ is the initial precision matrix reflecting the uncertainty of the target position expectation $\boldsymbol{\mu}_t^j$ with respect to the previous one $\boldsymbol{\mu}_{t-1}^j$. The state precision matrix $\boldsymbol{\lambda}_t^j$ is modelled by the Wishart distribution, with $\bar{\mathbf{V}}^j$ and \bar{n}^j denoting, respectively, its precision matrix and degrees of freedom. Note that $\bar{\cdot}$ denotes initial fixed parameter.

According to the general state evolution model defined above, the probability of the state evolution $p(\mathbf{x}_t^j | \mathbf{x}_{t-1}^j)$ is obtained by integrating over the mean $\boldsymbol{\mu}_t^j$ and the precision matrix $\boldsymbol{\lambda}_t^j$:

$$p(\mathbf{x}_t^j | \mathbf{x}_{t-1}^j) = \iint \mathcal{N}(\mathbf{x}_t^j | \boldsymbol{\mu}_t^j, \boldsymbol{\lambda}_t^j) p(\boldsymbol{\mu}_t^j, \boldsymbol{\lambda}_t^j | \mathbf{x}_{t-1}^j) d\boldsymbol{\mu}_t^j d\boldsymbol{\lambda}_t^j. \quad (4)$$

3.2. Observation model

The observation model depends on the sensing mode employed by the sensors. Considering data association ambiguity, we adopt the range-based mode for tracking precision, where the received signal strength indicator (RSSI) technology is employed for energy efficiency (He, Huang, Blum, Stankovic, and Abdelzاهر 2003). The RSSI determines the distance between a receiver, namely a sensor s of ID i (s^i), and a transmitter, the j -th target \mathbf{x}^j , based on the knowledge of a path-loss model ν . However, multi-path reflections, non line-of-sight conditions, and other shadowing effects lead to erroneous distance estimates. Therefore, a white Gaussian error $\epsilon_y^i \sim \mathcal{N}(0, \sigma_y^2)$ is introduced to model the shadowing. In addition, due to the noisy wireless link, the received signal at the CH is corrupted by a normally distributed noise $\epsilon^i \sim \mathcal{N}(0, \sigma_i^2)$. The measurements are formulated as follows:

$$y_t^{i,j} \sim \mathcal{N}(y_t^{i,j} | \nu^j(\mathbf{x}_t^j), \sigma_y^{-2}),$$

$$\text{where } \nu^j(\mathbf{x}_t^j) = \Psi_0 - 10\zeta \log \frac{\|\mathbf{s}^i - \mathbf{x}_t^j\|}{d_0}, \quad (5)$$

$$z_t^{i,j} = \begin{cases} \beta^i y_t^{i,j} + \epsilon^i, & \text{if } y_t^{i,j} \geq \gamma_s^i \\ \epsilon^i, & \text{otherwise} \end{cases}$$

where σ_y^2 is the variance of the shadowing ϵ_y^i . The signal power $\nu^j(\mathbf{x}_t^j)$ is a one-to-one mapping to the distance $\|\mathbf{s}^i - \mathbf{x}_t^j\|$ traveled by the signal. The other denotations are, respectively, d_0 the reference distance, Ψ_0 the known received signal power in dBm at d_0 , ζ the known path-loss distance exponent, which takes value in the range $[2, 4]$ ($\zeta = 2$ for propagation in free space, $\zeta = 4$ for relatively lossy environments and for the case of full specular reflection from the earth surface (Djurić, Vemula, Bugallo, and Míguez 2005)), β^i the attenuation coefficient associated with the sensor i . γ_s^i denotes the signal detection threshold of the sensor i , which is assumed to be identical for all the sensors and $\gamma_s^i = \Psi_0 - 10\zeta \log(r_s/d_0)$. Similarly, γ_c^i is the signal communication threshold of the sensor i , and $\gamma_c^i = \Psi_0 - 10\zeta \log(r_c/d_0)$. To update the estimate of the target j , the Bayesian filtering framework requires construction of an observation model $p(\mathbf{Z}_t | \mathbf{x}_t^j)$. Assuming that the noise samples ϵ^i are independently distributed, we have,

$$p(\mathbf{Z}_t | \mathbf{x}_t^j) = \prod_i [p(z_t^{i,j} | \mathbf{x}_t^j, y_t^{i,j} \geq \gamma_s^i) P(y_t^{i,j} \geq \gamma_s^i) + p(z_t^{i,j} | \mathbf{x}_t^j, y_t^{i,j} < \gamma_s^i) P(y_t^{i,j} < \gamma_s^i)]$$

$$= \prod_i [\mathcal{N}(z_t^{i,j} | \beta^i y_t^{i,j}, \sigma_z^{-2}) P(y_t^{i,j} \geq \gamma_s^i) + \mathcal{N}(z_t^{i,j} | 0, \sigma_z^{-2}) P(y_t^{i,j} < \gamma_s^i)], \quad (6)$$

$$\text{where } P(y_t^{i,j} \geq \gamma_s^i) = \int_{\gamma_s^i}^{\infty} \mathcal{N}(y_t^{i,j} | \nu^j(\mathbf{x}_t^j), \sigma_y^{-2}) dy_t^{i,j},$$

$$\text{and } P(y_t^{i,j} < \gamma_s^i) = 1 - P(y_t^{i,j} \geq \gamma_s^i).$$

The likelihood $p(\mathbf{Z}_t | \mathbf{x}_t^j)$ is fused with the state evolution model (4) within the Bayesian framework to estimate the temporal position of the target j .

An important problem introduced by the definition of the observation model $p(\mathbf{Z}_t | \mathbf{x}_t^j)$ is, the false alarm. One can note from the formulation (5) that the mapping between $\nu^j(\mathbf{x}_t^j)$ and $y_t^{i,j}$ is not deterministic, due to the shadowing effect of ϵ_y^i . That is to say, if $\nu^j(\mathbf{x}_t^j)$, the one-to-one mapping to the true distance $\|\mathbf{s}^i - \mathbf{x}_t^j\|$, is greater than the threshold γ_s^i , the observed measurement $y_t^{i,j}$ is not necessarily greater than γ_s^i . In fact, $P(y_t^{i,j} \geq \gamma_s^i)$ can also be formulated by

$$P(y_t^{i,j} \geq \gamma_s^i) = [p(y_t^{i,j} \geq \gamma_s^i | \nu^j(\mathbf{x}_t^j) \geq \gamma_s^i) P(\nu^j(\mathbf{x}_t^j) \geq \gamma_s^i) + p(y_t^{i,j} \geq \gamma_s^i | \nu^j(\mathbf{x}_t^j) < \gamma_s^i) P(\nu^j(\mathbf{x}_t^j) < \gamma_s^i)],$$

as shown in Figure 2. According to the Equation (6), the probability of false alarm $p(y_t^{i,j} \geq \gamma_s^i | \nu^j(\mathbf{x}_t^j) < \gamma_s^i)$ has already been naturally incorporated during the integral of Equation (6). Similarly, the symmetric probability of false alarm $p(y_t^{i,j} < \gamma_s^i | \nu^j(\mathbf{x}_t^j) \geq \gamma_s^i)$ is incorporated in the calculation of $P(y_t^{i,j} < \gamma_s^i)$.

4. Variational filtering for MTT

As the hidden state \mathbf{x}_t^j is extended to an augmented state $\boldsymbol{\alpha}_t^j = (\mathbf{x}_t^j, \boldsymbol{\mu}_t^j, \boldsymbol{\lambda}_t^j)$ by the Equation (3), the filtering distribution to be estimated thus takes the form of the joint *posterior* distribution $p(\boldsymbol{\alpha}_t^j | \mathbf{Z}_{1:t})$. A Variational Bayesian method is proposed for approximating the intractable integrals arising in Equation (1) and (2). Introducing a separable distribution $q(\boldsymbol{\alpha}_t^j)$, an analytical approximation to the *posterior* probability $p(\boldsymbol{\alpha}_t^j | \mathbf{Z}_{1:t})$ is provided by minimising the Kullback-Leibler divergence D_{KL} :

$$D_{\text{KL}}(q || p) = \int q(\boldsymbol{\alpha}_t^j) \log \left[\frac{q(\boldsymbol{\alpha}_t^j)}{p(\boldsymbol{\alpha}_t^j | \mathbf{Z}_{1:t})} \right] d\boldsymbol{\alpha}_t^j,$$

$$\text{where } q(\boldsymbol{\alpha}_t^j) = q(\mathbf{x}_t^j) q(\boldsymbol{\mu}_t^j) q(\boldsymbol{\lambda}_t^j).$$

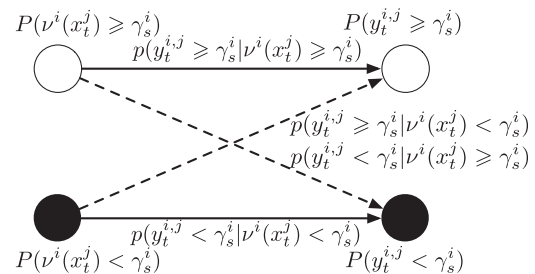


Figure 2. Probability model of the sensed observation $y_t^{i,j}$ with false alarms, where the dashed lines with arrows denote the false alarms.

To minimise D_{KL} subject to the constraint $\int q(\boldsymbol{\alpha}_t^j) d\boldsymbol{\alpha}_t^j = 1$, the Lagrange multiplier is used, yielding the following approximate distribution (Vermaak, Lawrence, and Pérez 2003b; Snoussi and Richard 2006; Teng et al. 2007a),

$$\begin{cases} q(\mathbf{x}_t^j) \propto \exp(\log p(\mathbf{Z}_{1:t}, \boldsymbol{\alpha}_t)) \prod q(\boldsymbol{\mu}_t^j) q(\boldsymbol{\lambda}_t^j) \\ q(\boldsymbol{\mu}_t^j) \propto \exp(\log p(\mathbf{Z}_{1:t}, \boldsymbol{\alpha}_t)) \prod q(\mathbf{x}_t^j) q(\boldsymbol{\lambda}_t^j), \\ q(\boldsymbol{\lambda}_t^j) \propto \exp(\log p(\mathbf{Z}_{1:t}, \boldsymbol{\alpha}_t)) \prod q(\boldsymbol{\mu}_t^j) q(\mathbf{x}_t^j) \end{cases} \quad (7)$$

where $\langle \cdot \rangle_q$ denotes the expectation operator relative to the distribution q . Taking into account the separable approximate distribution $q(\boldsymbol{\alpha}_{t-1}^j)$ at instant $t-1$, the predictive distribution $p(\boldsymbol{\alpha}_t^j | \mathbf{Z}_{1:t-1})$ and the filtering distribution $p(\boldsymbol{\alpha}_t^j | \mathbf{Z}_{1:t})$ are sequentially approximated according to the following scheme:

$$\begin{aligned} p(\boldsymbol{\alpha}_t^j | \mathbf{Z}_{1:t-1}) &\propto \int p(\boldsymbol{\alpha}_t^j | \boldsymbol{\alpha}_{t-1}^j) q(\boldsymbol{\alpha}_{t-1}^j) d\boldsymbol{\alpha}_{t-1}^j \\ &\propto p(\mathbf{x}_t^j, \boldsymbol{\lambda}_t^j | \boldsymbol{\mu}_t^j) q_p(\boldsymbol{\mu}_t^j) \\ p(\boldsymbol{\alpha}_t^j | \mathbf{Z}_{1:t}) &\propto p(\mathbf{Z}_t | \mathbf{x}_t^j) p(\boldsymbol{\alpha}_t^j | \mathbf{Z}_{1:t-1}) \\ &\propto p(\mathbf{Z}_t | \mathbf{x}_t^j) p(\mathbf{x}_t^j, \boldsymbol{\lambda}_t^j | \boldsymbol{\mu}_t^j) q_p(\boldsymbol{\mu}_t^j), \end{aligned} \quad (8)$$

$$\text{where } q_p(\boldsymbol{\mu}_t^j) = \int p(\boldsymbol{\mu}_t^j | \boldsymbol{\mu}_{t-1}^j) q(\boldsymbol{\mu}_{t-1}^j) d\boldsymbol{\mu}_{t-1}^j.$$

Therefore, through a simple integral with respect to $\boldsymbol{\mu}_{t-1}^j$, the predictive and the filtering distributions involved in the Bayesian inference can be sequentially updated. Considering the GSEM proposed in Equation (3), the evolution of $\boldsymbol{\mu}_{t-1}^j$ is Gaussian, namely $p(\boldsymbol{\mu}_t^j | \boldsymbol{\mu}_{t-1}^j) \sim \mathcal{N}(\boldsymbol{\mu}_{t-1}^j, \bar{\boldsymbol{\lambda}}^j)$. Defining $q(\boldsymbol{\mu}_{t-1}^j) \sim \mathcal{N}(\boldsymbol{\mu}_{t-1}^{j,*}, \boldsymbol{\lambda}_{t-1}^{j,*})$, $q_p(\boldsymbol{\mu}_t^j)$ is also Gaussian, with the following parameters,

$$q_p(\boldsymbol{\mu}_t^j) \sim \mathcal{N}(\boldsymbol{\mu}_t^{p,j}, \boldsymbol{\lambda}_t^{p,j}),$$

$$\text{where } \boldsymbol{\mu}_t^{p,j} = \boldsymbol{\mu}_{t-1}^{j,*}, \text{ and } \boldsymbol{\lambda}_t^{p,j} = [(\boldsymbol{\lambda}_{t-1}^{j,*})^{-1} + (\bar{\boldsymbol{\lambda}}^j)^{-1}]^{-1}. \quad (9)$$

The temporal dependence is hence reduced to the incorporation of only one Gaussian component approximation $q(\boldsymbol{\mu}_{t-1}^j)$ for the target j . The update and the approximation of the filtering distribution $p(\boldsymbol{\alpha}_t^j | \mathbf{Z}_{1:t})$ are jointly performed, yielding a natural and adaptive compression (Snoussi and Richard 2006; Teng, Snoussi, and Richard 2010). According to Equation (7), variational calculus leads to closed-form expressions of $q(\boldsymbol{\mu}_t^j)$ and $q(\boldsymbol{\lambda}_t^j)$, by substituting the deduction Equations (9) into Equation (8):

$$q(\boldsymbol{\mu}_t^j) \sim \mathcal{N}(\boldsymbol{\mu}_t^{j,*}, \boldsymbol{\lambda}_t^{j,*}), \quad q(\boldsymbol{\lambda}_t^j) \sim \mathcal{W}_{n_x}(\mathbf{V}^{j,*}, n^{j,*}),$$

Similarly, the expectations involved in the predictive distribution $p(\boldsymbol{\alpha}_t^j | \mathbf{Z}_{1:t-1})$ also have closed forms:

$$\begin{cases} q_{t|t-1}(\mathbf{x}_t^j) \propto \mathcal{N}(\langle \boldsymbol{\mu}_t^j \rangle_{q_{t|t-1}}, \langle \boldsymbol{\lambda}_t^j \rangle_{q_{t|t-1}}) \\ q_{t|t-1}(\boldsymbol{\mu}_t^j) \propto \mathcal{N}(\boldsymbol{\mu}_{t|t-1}^{j,*}, \boldsymbol{\lambda}_{t|t-1}^{j,*}) \\ q_{t|t-1}(\boldsymbol{\lambda}_t^j) \propto_{n_x} (\mathbf{V}_{t|t-1}^{j,*}, n_{t|t-1}^{j,*}) \end{cases} \quad (10)$$

Therefore, the computational cost and the memory requirements are dramatically reduced by the variational approximation in the prediction phase. In fact, the expectations involved in the computation of the predictive distribution have closed forms, avoiding the use of Monte Carlo integration.

On the other hand, the update and the approximation of the filtering distribution $p(\boldsymbol{\alpha}_t^j | \mathbf{Z}_{1:t})$ are simultaneously performed. By combining the Equation (7) and (8), we have the following form,

$$\begin{aligned} p(\boldsymbol{\alpha}_t^j | \mathbf{Z}_{1:t}) &\approx q(\boldsymbol{\alpha}_t^j) = q(\mathbf{x}_t^j) q(\boldsymbol{\mu}_t^j) q(\boldsymbol{\lambda}_t^j), \\ \text{where } &\begin{cases} q(\mathbf{x}_t^j) \propto p(\mathbf{Z}_t | \mathbf{x}_t^j) \mathcal{N}(\langle \boldsymbol{\mu}_t^j \rangle, \langle \boldsymbol{\lambda}_t^j \rangle) \\ q(\boldsymbol{\mu}_t^j) \propto \mathcal{N}(\boldsymbol{\mu}_t^{j,*}, \boldsymbol{\lambda}_t^{j,*}) \\ q(\boldsymbol{\lambda}_t^j) \propto_{n_x} (\mathbf{V}^{j,*}, n^{j,*}) \end{cases}, \end{aligned} \quad (11)$$

where the state evolution model (3) and the observation model (5) are incorporated to update $q(\mathbf{x}_t^j)$. However, due to the incorporation of observations, the estimate of target state \mathbf{x}_t^j does not have a tractable form, which immediately suggests an Importance Sampling (IS) procedure:

$$\begin{aligned} \mathbf{x}_t^{j,(k)} &\sim \mathcal{N}(\langle \boldsymbol{\mu}_t^j \rangle, \langle \boldsymbol{\lambda}_t^j \rangle), \quad \forall k = 1, \dots, N \\ w_t^{j,(k)} &\propto \begin{cases} p(\mathbf{Z}_t | \mathbf{x}_t^{j,(k)}), \\ \text{if targets are far apart} \\ p(\mathbf{Z}_t^{\text{amb}} | \mathbf{x}_t^{j,(k)}) p(\mathbf{Z}_t \setminus \mathbf{Z}_t^{\text{amb}} | \mathbf{x}_t^{j,(k)}), \\ \text{otherwise} \end{cases}, \quad (12) \\ \langle \mathbf{x}_t^j \rangle &= \sum_{k=1}^N w_t^{j,(k)} \mathbf{x}_t^{j,(k)}. \end{aligned}$$

Let $\mathbf{Z}_t^{\text{amb}}$ denote the set of ambiguous observations. When the targets to be tracked are far apart, namely $\mathbf{Z}_t^{\text{amb}} = \emptyset$, observations \mathbf{Z}_t are directly incorporated to update target estimates. Otherwise, the SMCDA phase is invoked to compute $p(\mathbf{Z}_t^{\text{amb}} | \mathbf{x}_t^{j,(k)})$, $\forall j = 1, \dots, M$, whereas the other observations $\mathbf{Z}_t \setminus \mathbf{Z}_t^{\text{amb}}$ are directly incorporated by the VF. During the execution of the VF, the update and the approximation of the filtering distribution $p(\boldsymbol{\alpha}_t^j | \mathbf{Z}_{1:t})$ are jointly performed, yielding a natural and adaptive compression of a Gaussian distribution for each target. One can note that the main advantage of the variational approach is the compression of the statistics required to update the filtering distribution between two successive instants. Thanks to

the variational calculus, communication between CH_{t-1} and CH_t is limited to simply sending the mean and the covariance of $q(\mu_{t-1})^j$, despite of the non-closed form of $q(\mathbf{x}_{t-1})^j$. On the contrary, the classical SMC algorithm maintains and propagates a large number of particles and their corresponding weights. What is more important, since approximation of the filtering distribution is performed during the measurement incorporation, the error propagation is dramatically reduced by the VF. This implicit compression makes the VF algorithm much more adapted to distributed implementation in WSNs. The pseudo-code of the extended VF for multi-target tracking is listed in Algorithm 1.

Algorithm 1: Extended variational filter for multi-target tracking

Input: \mathbf{Z}_t , $\{\bar{\lambda}^j\}_{j=1}^M$, $\{\bar{\mathbf{V}}^j\}_{j=1}^M$, $\{\bar{n}^j\}_{j=1}^M$, $\{q(\mu_0^j)\}_{j=1}^M \sim \{\mathcal{N}(\mu_0^{j,*}, \lambda_0^{j,*})\}_{j=1}^M$

Output: $\langle X_t \rangle$

for $t = 1, 2, \dots$ **do**

for $j = 1, \dots, M$ **do**

 Predict $p(\alpha_t^j | \mathbf{Z}_{1:t-1}) \propto p(\mathbf{x}_t^j, \lambda_t^j | \mu_t^j) q_p(\mu_t^j)$;

while not converge do

 Calculate the hyper parameters involved in Equation (10):

$$\mu_t^{j,p} = \mu_{t-1}^{j,*}, \lambda_t^{j,p} = (\lambda_{t-1}^{j,*-1} + \bar{\lambda}^{j-1})^{-1}, n_{t|t-1}^{j,*} = \bar{n}^j + 1,$$

$$\mu_{t|t-1}^{j,*} = \lambda_{t|t-1}^{j,*-1} (\langle \lambda_t^j \rangle_{q_{t|t-1}} \langle \mathbf{x}_t^j \rangle_{q_{t|t-1}} + \lambda_t^{j,p} \mu_t^{j,p}),$$

$$\lambda_{t|t-1}^{j,*} = \langle \lambda_t^j \rangle_{q_{t|t-1}} + \lambda_t^{j,p},$$

$$\begin{aligned} \mathbf{V}_{t|t-1}^{j,*} = & (\langle \mathbf{x}_t^j \mathbf{x}_t^{j,T} \rangle_{q_{t|t-1}} - \langle \mathbf{x}_t^j \rangle_{q_{t|t-1}} \langle \mu_t^j \rangle_{q_{t|t-1}}^T \\ & - \langle \mu_t^j \rangle_{q_{t|t-1}} \langle \mathbf{x}_t^j \rangle_{q_{t|t-1}}^T + \left\langle \mu_t^j \mu_t^{j,T} \right\rangle_{q_{t|t-1}} + \bar{\mathbf{V}}^{j-1})^{-1}; \end{aligned}$$

end

 The predicted expectation $\langle \mathbf{x}_t^j \rangle_{q_{t|t-1}} = \langle \mu_t^j \rangle_{q_{t|t-1}}$;

if hand-off then

 Select the new CH_t^j by residual energy comparison;

 Communicate $q(\mu_{t-1}^j)$ to the new CH_t^j ;

else

$\text{CH}_t^j = \text{CH}_{t-1}^j$, replace the storage of particles by $q(\mu_{t-1}^j)$;

end

end

if $N_{amb} > 3$ **then**

 Cluster merging;

 SMCDA to incorporate $p(\mathbf{Z}_t^{amb} | X_t)$, and

$$\hat{X}_t = \sum_{k=1}^N \hat{W}_t^{(k)} \mathbf{x}_t^{(k)};$$

end

for $j = 1, \dots, M$ **do**

if $N_{amb} > 3$ **then**

$\mu_t^{j,*} = \sum_{k=1}^N \hat{W}_t^{(k)} \mathbf{x}_t^{j,(k)}$, the component j of estimate in SMCDA;

else

$$\mu_t^{j,*} = \mu_t^{j,p}, \lambda_t^{j,*} = 2\lambda_t^{j,p};$$

end

while not converge do

 Calculate the hyper-parameters to update $p(\alpha_t^j | \mathbf{Z}_{1:t})$:

$$\langle \mu_t^j \rangle = \mu_t^{j,*}, \langle \lambda_t^j \rangle = n^{j,*} \mathbf{V}^{j,*}$$

$$\mu_t^{j,*} = \lambda_t^{j,*-1} (\langle \lambda_t^j \rangle \langle \mathbf{x}_t^j \rangle + \lambda_t^{j,p} \mu_t^{j,p}),$$

$$\lambda_t^{j,*} = \langle \lambda_t^j \rangle + \lambda_t^{j,p}, \quad n^{j,*} = \bar{n}^j + 1,$$

$$\begin{aligned} \mathbf{V}^{j,*} = & (\langle \mathbf{x}_t^j \mathbf{x}_t^{j,T} \rangle - \langle \mathbf{x}_t^j \rangle \langle \mu_t^j \rangle^T - \langle \mu_t^j \rangle \langle \mathbf{x}_t^j \rangle^T \\ & + \langle \mu_t^j \mu_t^{j,T} \rangle + \bar{\mathbf{V}}^{j-1})^{-1}; \end{aligned}$$

end

 Sample $\{\mathbf{x}_t^{j,(k)}, w_t^{j,(k)}\}_{k=1}^N$ from $q(\mathbf{x}_t^j)$ according to Equation (12);

if $\hat{N}_{eff} = \frac{1}{\sum_{k=1}^N (w_t^{j,(k)})^2} < N_{threshold}$ **then**

 Resampling;

end

 Compute the expectation $\langle \mathbf{x}_t^j \rangle = \sum_{k=1}^N w_t^{j,(k)} \mathbf{x}_t^{j,(k)}$;

end

 Return $\langle X_t \rangle = \{\langle \mathbf{x}_t^j \rangle\}_{j=1}^M$;

end

5. Probabilistic data association

As mentioned above, for the sake of resource efficiency, the data association phase is only invoked when dealing with ambiguous observations \mathbf{Z}_t^{amb} . Since each target is tracked by a cluster of sensors, cluster merging is necessary to incorporate ambiguous measurements when targets are moving closely. A new and larger cluster is thus formed to process the measurements generated by the encountering targets. In the following, a detailed description of the probabilistic data association phase is given.

5.1. Cluster merging

The cluster merging phase is independent of the clustering protocol employed for MTT. In fact, the new CH leader for data association is selected based on residual energy comparison of the neighbouring CHs. We assume that each CH is capable of detecting its own residual energy level. The comparison of residual energy is performed by information exchange among the neighbouring CHs. Figure 3(a) and (b) illustrate the tracking of two crossing targets in a WSN. The field under surveillance is covered by sensors marked with small circles. Each sensor measures the signal energy from any target within its sensing range r_s , together with some random background noises

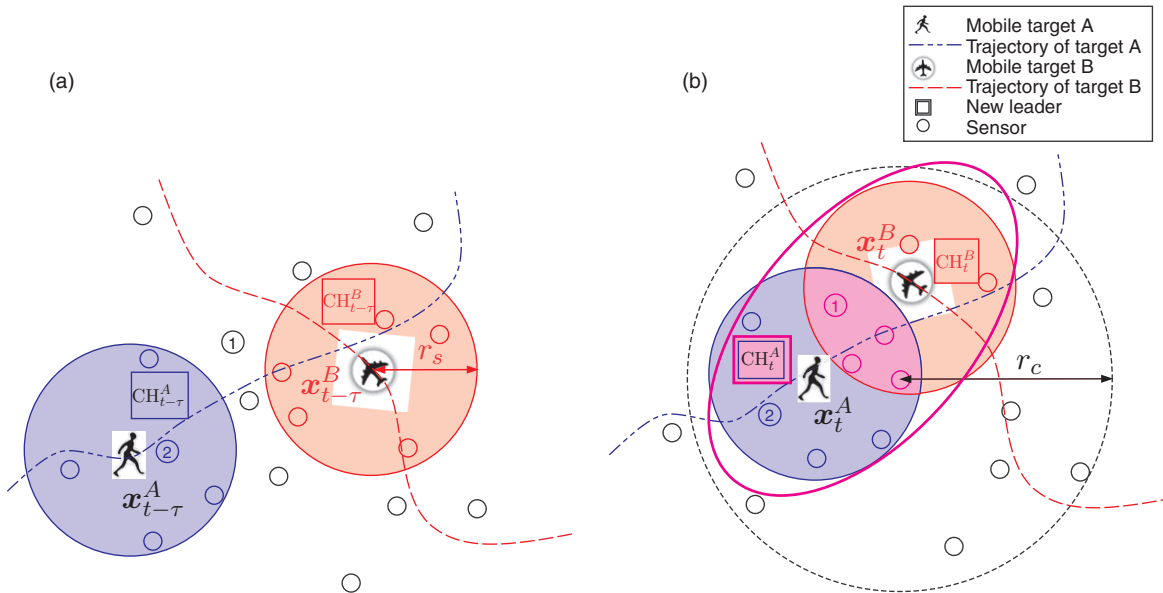


Figure 3. Example of tracking two crossing targets. (a) Snapshot of Multi-target tracking scenario at instant $t - \tau$. The target A and the target B are far apart, and are tracked, respectively, by different clusters and (b) Snapshot of Multi-target tracking scenario at instant t . The target A and the target B are moving closer, resulting data association ambiguity.

modelled by independent white Gaussian noises. Initially, the targets are well separated and are tracked by different clusters, visualised in red and blue colors, respectively in Figure 3. Sensors within the sensing range r_s , shown as disks centred at the target locations, transfer their observations to the corresponding CHs ($CH_{t-\tau}^A$ and $CH_{t-\tau}^B$). The CHs are in charge of collecting measurements from the cluster members, updating the estimate and maintaining the cluster structure. When the two targets move closely, their clusters collide. The collision is flagged when a sensor finds itself led by two distinct CHs (see the sensor identified by the number ‘1’ in Figure 3(b) for example). To demonstrate the collision, the colour of the overlapped sensors is also blended to purple. At this time, tracking switches to MTT mode, and the two clusters merge into one cluster, denoted by the purple ellipse in Figure 3(b). The CH of the more residual energy in the original two clusters is elected to be the new leader. In the specific case illustrated in Figure 3(b), the new leader is the original $CH_{t-\tau}^A$. The observations collected at $CH_{t-\tau}^B$ are transferred to the new leader for further processing. As mentioned in Section 2, the configuration of the sensor network guarantees that the distances between the sensors detecting a same target are smaller than r_c , as shown in Figure 3(b). It is therefore reasonable to assume that the CH with data association ambiguity only needs to communicate with its neighbouring CHs to collect a complete set of ambiguous measurements. All the measurements of the instant t , denoted by Z_t , are

collected at the new leader. As shown in Figure 3(b), only the sensors within the overlapped area (denoted by the small purple circles) can detect both targets at the same time. Their observations are also much more vulnerable to collisions and clutters in the wireless links. We use Z_t^{amb} to denote the set of measurements observed by these sensors. If the number N_{amb} of measurements in Z_t^{amb} is smaller than three and the number of $Z_t \setminus Z_t^{\text{amb}}$ is greater than three, we simply discard the ambiguous observations for energy efficiency. In this case, the targets are tracked respectively using the rest observations $Z_t \setminus Z_t^{\text{amb}}$, since they can be simply distinguished and assigned to the specific targets. On the other hand, if $N_{\text{amb}} > 3$, the data association phase is invoked in the new CH to assign the ambiguous measurements using the SMC method. Besides the SMCDA phase, the rest of the observations $Z_t \setminus Z_t^{\text{amb}}$ are incorporated by the VF algorithm to refine the target estimates.

5.2. SMC data association

The ambiguous observation vector Z_t^{amb} is composed of detection measurements and clutter measurements, where the latter are assumed to be uniformly distributed in the observation area. In addition, some assumptions are commonly made for the data association problem (Bar-Shalom and Fortmann 1988):

- (1) One measurement can originate from one target or from the clutter.

- (2) One target can produce zero or one signal at one time. Since one target is sensed by at least three sensors at a time, measurements observed by different sensors could be generated by the same signal of a target. On the contrary, the measurements observed by a single sensor at one time come from different targets or clutters.

As the origin of each measurement is unknown, a vector \mathbf{K}_t is introduced to describe the associations between the measurements and the targets. Each component of \mathbf{K}_t is a random variable taking its values in $\{0, \dots, M\}$, where 0 is dedicated to the clutter. Assuming the total amount of ambiguous observations is N_{amb} , the set of ambiguous observations is denoted by $\mathbf{Z}_t^{\text{amb}} = \{Z_t^{i_{\text{amb}}}\}_{i_{\text{amb}}=1}^{N_{\text{amb}}}$. Accordingly, $\mathbf{K}_t^{\text{amb}} = \{K_t^{i_{\text{amb}}}\}_{i_{\text{amb}}=1}^{N_{\text{amb}}}$, where $K_t^{i_{\text{amb}}} = j$ indicates that $Z_t^{i_{\text{amb}}}$ is associated with the target j . In this case, $\mathbf{Z}_t^{\text{amb}}$ is a realisation of the stochastic process:

$$Z_t^{i_{\text{amb}}} = H_t^{j, i_{\text{amb}}}(\mathbf{x}_t^j, \sigma_t^{j, i_{\text{amb}}}) \quad \text{if } K_t^{i_{\text{amb}}} = j. \quad (13)$$

The noise $\sigma_t^{j, i_{\text{amb}}}$ is assumed to be a white noise independent of the other observation noises. We assume that the hypothesis $H_t^{j, i_{\text{amb}}}$ can be associated with a functional form $F(Z_t^{i_{\text{amb}}}; \mathbf{x}_t^j)$ such that,

$$F(Z_t^{i_{\text{amb}}}; \mathbf{x}_t^j) \propto p(Z_t^{i_{\text{amb}}} | \mathbf{x}_t^j, K_t^{i_{\text{amb}}} = j). \quad (14)$$

If $K_t^{i_{\text{amb}}} = 0$, the measurement $Z_t^{i_{\text{amb}}}$ is associated with the clutter. As the indexing of the ambiguous measurements is arbitrary, all the measurements have the same *a priori* probability to be associated with a given target j . For each ambiguous measurement, a vector $\Pi_t = \{\pi_t^j\}_{j=0}^M \in [0, 1]^{M+1}$ is defined for the association probability, where π_t^j is a discrete probability that any measurement is associated with the target j . With respect to the two general assumptions mentioned above, the first one expresses that the association is exclusive and exhaustive. Accordingly, $\sum_{j=0}^M \pi_t^j = 1$. The second assumption implies that N_{amb} may differ from M and that the association variables $K_t^{i_{\text{amb}}}$ for $i_{\text{amb}} = 1, \dots, N_{\text{amb}}$ are dependent.

The number of clutter measurements is assumed to be distributed according to a Poisson distribution of parameter aS , where S is the size of the observation area, and a is the number of clutter measurements per area unit. The association probability π_t^0 that a measurement is associated with a clutter is a constant and can be computed as follows,

$$\begin{aligned} \pi_t^0 &= \sum_{l=0}^{N_{\text{amb}}} P(K_t^{i_{\text{amb}}} = 0 | N_t^0 = l) P(N_t^0 = l) \\ &= \sum_{l=0}^{N_{\text{amb}}} \frac{l}{N_{\text{amb}}} \exp(-aS) \frac{(aS)^l}{l!}, \end{aligned} \quad (15)$$

where N_t^0 is the number of measurements arising from the clutter at time t . Assuming that there are l clutter measurements among the N_{amb} measurements, the *a priori* probability that any measurement comes from the clutter is equal to l/N_{amb} . Thus, we get the equality $P(K_t^{i_{\text{amb}}} = 0 | N_t^0 = l) = l/N_{\text{amb}}$. The distribution of clutter follows a Poisson distribution of parameter aS , thus $P(N_t^0 = l) = \exp(-aS) \frac{(aS)^l}{l!}$.

The data association phase is initialised by generating a set of N particles $\mathbf{X}_t = \{\mathbf{x}_t^{(k)}, w_t^{(k)}\}_{k=1}^N$. For all $k = 1, \dots, N$, the likelihood of the particles are formulated as:

$$\begin{aligned} p(\mathbf{Z}_t^{\text{amb}} | \mathbf{x}_t^{(k)}) &= \prod_{i_{\text{amb}}=1}^{N_{\text{amb}}} p(Z_t^{i_{\text{amb}}} | \mathbf{x}_t^{(k)}) \\ &\propto \prod_{i_{\text{amb}}=1}^{N_{\text{amb}}} \left[\frac{\pi_t^0}{S} + \sum_{j=1}^M F(Z_t^{i_{\text{amb}}}; \mathbf{x}_t^{j, (k)}) \pi_t^j \right]. \end{aligned} \quad (16)$$

The vectors \mathbf{X}_t , \mathbf{K}_t and Π_t are random variables with known prior distributions. Samples are then obtained iteratively from their joint posterior using a proper Markov Chain Monte Carlo (MCMC) technique, namely, the Gibbs sampler (Hue et al. 2002a). Denoting as $\Theta_t = (\mathbf{X}_t, \mathbf{K}_t, \Pi_t)$, the Gibbs algorithm consists of generating a Markov chain that converges to the distribution $p(\Theta_t | \mathbf{Z}_t^{\text{amb}})$, which cannot be sampled directly. In order to implement the Gibbs sampler, we choose the following partition:

$$\begin{cases} \Theta_t^{i_{\text{amb}}} = K_t^{i_{\text{amb}}}, & \text{for } i_{\text{amb}} = 1, \dots, N_{\text{amb}} \\ \Theta_t^{N_{\text{amb}}+j} = \pi_t^j, & \text{for } j = 1, \dots, M \\ \Theta_t^{N_{\text{amb}}+M+j} = \mathbf{x}_t^j, & \text{for } j = 1, \dots, M \end{cases}. \quad (17)$$

The initialisation of the Gibbs sampler consists of assigning uniform association probabilities, i.e. $\bar{\Pi}_t = \{\pi_t^j = (1 - \pi_t^0)/M\}_{j=1}^M$, and using the predictive target positions Equation (10) to initialise $\bar{\mathbf{X}}_t = \{\{\mathbf{x}_t^j\}_{q|t-1}\}_{j=1}^M$. The \mathbf{K}_t variables do not need initialisation as they are sampled conditioned on Π_t and \mathbf{X}_t at the first step of the Gibbs sampler. After a finite number of iterations, estimations of the random variables are obtained, namely $\hat{\Theta}_t = (\hat{\mathbf{X}}_t, \hat{\mathbf{K}}_t, \hat{\Pi}_t)$. Therefore, the ambiguous observations are assigned by $\hat{\mathbf{K}}_t$, and are incorporated to update the target estimates $\hat{\mathbf{X}}_t$. The particles $\{\mathbf{X}_t^{(k)}, \hat{W}_t^{(k)}\}_{k=1}^N$ generated by the data association phase are directly employed to incorporate the rest of observations $\mathbf{Z}_t \setminus \mathbf{Z}_t^{\text{amb}}$, according to Equation (12). Each particle $\mathbf{X}_t^{(k)}$ is a vector of dimension $n_x \times M$, where we denote by $\mathbf{x}_t^{j, (k)}$ the j -th component of particle $\mathbf{X}_t^{(k)}$. The estimation $\hat{\mathbf{x}}_t^j = \sum_{k=1}^N \hat{w}_t^{j, (k)} \mathbf{x}_t^{j, (k)}$ is used to initialise the VF of the target j . After the run of the VF algorithm, estimates on the targets are refined, especially the distributions of the particles are naturally approximated by a simple

Gaussian distribution for each target. The pseudo-code of the collaborative MTT scheme is summarised in the Algorithm 2.

Algorithm 2: Collaborative multi-target tracking scheme

Input: \mathbf{Z}_t , $\{\bar{\lambda}^j\}_{j=1}^M$, $\{\bar{\nu}^j\}_{j=1}^M$, $\{\bar{n}^j\}_{j=1}^M$, $\{q(\mu_0^j)\}_{j=1}^M \sim \{\mathcal{N}(\mu_0^{j,*}, \lambda_0^{j,*})\}_{j=1}^M$

Output: $\langle X_t \rangle$

for $t = 1, 2, \dots$ **do**

for $j = 1, \dots, M$ **do**

Predict $p(\mathbf{x}_t^j | \mathbf{Z}_{1:t-1}) \propto p(\mathbf{x}_t^j, \lambda_t^j | \mu_t^j) q_p(\mu_t^j)$;

while not converge do

Calculate the hyper parameters involved in $q_{t|t-1}(\mathbf{x}_t^j)$ of Equation (10);

end

Predictive expectation $\langle \mathbf{x}_t^j \rangle_{q_{t|t-1}} = \langle \mu_t^j \rangle_{q_{t|t-1}}$;

if hand-off then

Select the new CH_t^j by residual energy comparison;

Communicate $q(\mu_{t-1}^j)$ to the new CH_t^j ;

else

$\text{CH}_t^j = \text{CH}_{t-1}^j$, replace the storage of particles by $q(\mu_{t-1}^j)$;

end

end

if $N_{amb} > 3$ **then**

New leader election by residual energy comparison among $\{\text{CH}_t^j\}_{j=1}^M$;

Cluster merging to collect the complete set of observations \mathbf{Z}_t ;

Initialise of the Gibbs sampler:

$$\bar{\Pi}_t = \{\bar{\pi}_t^j\}_{j=0}^M, \text{ where } \bar{\pi}_t^0 = \sum_{l=0}^{N_{amb}} \frac{l}{N_{amb}} \exp(-aS) \frac{(aS)^l}{l!},$$

$$\bar{\pi}_t^j = (1 - \bar{\pi}_t^0) / M$$

$$\bar{\mathbf{X}}_t = \{\bar{\mathbf{x}}_t^j\}_{j=1}^M = \left\{ \sum_{k=1}^N \mathbf{x}_t^{j(k)} w_t^{j(k)} \right\}_{j=1}^M = \{\langle \mathbf{x}_t^j \rangle_{q_{t|t-1}}\}_{j=1}^M,$$

where $\mathbf{x}_t^{j(k)} \sim \mathcal{N}(\langle \mu_t^j \rangle_{q_{t|t-1}}, \langle \lambda_t^j \rangle_{q_{t|t-1}})$,

$$\mathbf{W}_t^{(k)} = \{w_t^{j(k)}\}_{j=1}^M = \{1/(NM)\}_{j=1}^M$$

Run of Gibbs sampler to estimate random variables $\hat{\Theta}_t = (\hat{\mathbf{X}}_t, \hat{\mathbf{K}}_t, \hat{\Pi}_t)$;

Incorporation of the ambiguous observations by SMCDA:

$$\hat{\mathbf{X}}_t = \sum_{k=1}^N \hat{W}_t^{(k)} \mathbf{X}_t^{(k)} = \sum_{k=1}^N p(\mathbf{Z}_t^{\text{amb}} | \mathbf{X}_t^{(k)}) \mathbf{X}_t^{(k)};$$

end

for $j = 1, \dots, M$ **do**

if $N_{amb} > 3$ **then**

Initialise $\mu_t^{j,*} = \hat{\mathbf{x}}_t^j = \sum_{k=1}^N \hat{w}_t^{j(k)} \mathbf{x}_t^{j(k)}$;

Recursively update the hyper parameters of VF; Directly employ the particles of SMCDA to incorporate $\mathbf{Z}_t \setminus \mathbf{Z}_t^{\text{amb}}$

$$\mathbf{x}_t^{j(k)} \sim \mathcal{N}(\hat{\mathbf{x}}_t^j, \langle \lambda_t^j \rangle), \quad w_t^{j(k)} = \hat{w}_t^{j(k)} p(\mathbf{Z}_t \setminus \mathbf{Z}_t^{\text{amb}} | \mathbf{x}_t^{j(k)}), \\ \forall k = 1, \dots, N;$$

else

Initialise $\mu_t^{j,*} = \mu_t^{j,p}$, $\lambda_t^{j,*} = 2\lambda_t^{j,p}$;

Recursively update the hyper parameters of VF; Generate new particles $\{\mathbf{x}_t^{j(k)}, w_t^{j(k)}\}_{k=1}^N$ to incorporate $\mathbf{Z}_t \setminus \mathbf{Z}_t^{\text{amb}}$

$$\mathbf{x}_t^{j(k)} \sim \mathcal{N}(\langle \mu_t^j \rangle, \langle \lambda_t^j \rangle), \quad w_t^{j(k)} = p(\mathbf{Z}_t \setminus \mathbf{Z}_t^{\text{amb}} | \mathbf{x}_t^{j(k)}), \\ \forall k = 1, \dots, N;$$

end

Compute the expectation $\langle \mathbf{x}_t^j \rangle = \sum_{k=1}^N w_t^{j(k)} \mathbf{x}_t^{j(k)}$;

end

Return $\langle X_t \rangle = \{\langle \mathbf{x}_t^j \rangle\}_{j=1}^M$;

end

6. Hypothesis testing for varying number of targets

The number of targets M is assumed to be known and constant until now. However, this assumption is not always true in real world situations. In fact, by assuming the number M of targets to be tracked is a discrete variable, the above collaborative MTT scheme can be extended to much more general situations. As far as the proposed distributed scheme is concerned, this extension consists of updating M and adding/removing the components of the particles related to the arrival/disappearance of targets. If the targets are far apart, the appearance of a new target can be simply detected by the number of new measurements generated at the same instant. As the three-coverage requirement has been guaranteed by the deployment of sensors, if more than three sensors in the neighbourhood report the detection of a new target at a time, a new VF is initialised to track the target. Similarly, the number of measurements N_t^j related to a known target j is used to confirm its disappearance. If N_t^j drops sharply for successive sampling instants, we assume the target j disappears from the surveillance area.

The difficulty arises when the number of targets varies in the joint space of targets, where the targets are in close proximity to each other. If a new target appears in the joint space of crossing targets, there is a great chance that the new target is considered as the clutter by the data association phase. Hue et al. (2002a) proposed to use the values of the assignment variables \mathbf{K}_t to make decision on the appearance of a new target. They assume that the arrival of a new target might be related to an

ambiguous observation $Z_t^{i\text{amb}}$ of low likelihood, whatever the target is associated with. As a result, the assignment variable $K_t^{i\text{amb}}$ of the observation $Z_t^{i\text{amb}}$ simulated by the Gibbs sampler might be more often equal to 0, namely the clutter. A χ^2 test is adopted to measure the adequation between the assumed Poisson law and the empirical law of the clutter estimated by $N_t^0 = \#\{K_t^{i\text{amb}} = 0\}$. However, Hue et al. have admitted that the initialisation of the new target based on the observation set is a tricky problem that they have not solved yet (Hue et al. 2002a). Generally speaking, the targets to be tracked are of distinct velocities and trajectories, leading to rare occurrence and short duration of joint target tracking. It is thus reasonable to assume that only one new target arrives at a time when the targets are crossing. As far as the assumptions proposed in Section 5.2 are concerned, we can detect the arrival of a new target by simply re-checking the assignment of measurements made in the SMCDA phase. As mentioned above, the data association phase only performs on the ambiguous observations Z_t^{amb} for energy efficiency. In the Section 5.2, the set of ambiguous observations is defined as $Z_t^{\text{amb}} = \{Z_t^{i\text{amb}}\}_{i=1}^{N_{\text{amb}}}$, where N_{amb} denotes the number of the observations in the set. With respect to the sensors, Z_t^{amb} can also be defined as $Z_t^{\text{amb}} = \{z_t^{i'} | z_t^{i'} = \{z_t^{i_1}, z_t^{i_2}, \dots\}\}_{i'=1}^{N_t^s}$, where N_t^s denotes the number of sensors with several observations at instant t . According to the assumptions made in the Section 5.2, the measurements $z_t^{i'}$ could be generated by either the targets or clutter. Assuming that a subset of observations $z_t^{i_{\text{target}}}$ are assigned to the targets, the other observations $z_t^{i'} \setminus z_t^{i_{\text{target}}}$ are associated with clutter. With respect to all the assumptions mentioned above, we assume that a new target appears in the joint space of the crossing targets, if and only if the following conditions are satisfied:

- The number of measurements $N_t^{i_{\text{clutter}}}$ in the set $z_t^{i'} \setminus z_t^{i_{\text{target}}}$ is greater than a threshold $N_{\text{threshold}}^{\text{clutter}}$, namely $N_t^{i_{\text{clutter}}} > N_{\text{threshold}}^{\text{clutter}}$.
- The number of sensors with the same situation $N_t^{s'} = \#\{i' | N_t^{i_{\text{clutter}}} > N_{\text{threshold}}^{\text{clutter}}\}$ is more than three, namely $N_t^{s'} > 3$. As the deployment of sensors guarantees the three-coverage requirement, the newly arrived target could also be detected by at least 3 sensors at a time.

Therefore, a simple and effective comparison instead of the hypothesis test of Hue et al. (2002a) is employed in our strategies, for deciding a new arrival in the intersection space of target trajectories. If a new arrival is confirmed, the SMCDA process has to be performed once again on the set of observations Z_t to handle potential confusions between all the $M+1$ targets and the clutter. Concerning the initialisation stage of the

SMCDA process, \bar{x}_t^{new} is assumed to be the centroid of the sensors used for its detection.

On the other hand, the disappearance of an identified (tracked) target j in the WSN is decided by the number of measurements N_t^j related to it. When the targets are far apart, N_t^j is simply equal to the number of sensors in the corresponding cluster implementing the tracking of the target j . In the case when the targets are close to each other, N_t^j is calculated by the data association phase. If N_t^j drops sharply for successive sampling instants, we assume the target j disappears from the surveillance area. We employ the hypothesis testing method proposed in Hue et al. (2002a) to detect disappearance of a target with data association ambiguity. As defined in Section 5.2, π_t^j describes the discrete probability that any measurement is associated with the target j . Thus, the disappearance of the target j from the surveillance area could be detected by a drop in the corresponding π_t^j component. However, the drop of the value of π_t^j may also be due to the failure of sensor detection, which is assumed to occur with a probability p_{fail} . Therefore, the detection of the target j can be viewed as a variable D_t^j distributed according to a binomial law of parameters $(1 - p_{\text{fail}}, p_{\text{fail}})$. By defining a threshold $D_{\text{threshold}}$, the value of D_t^j can be simply assigned as follows:

$$\begin{cases} \hat{D}_t^j = 1, & \text{if } \hat{\pi}_t^j \geq D_{\text{threshold}} \\ \hat{D}_t^j = 0, & \text{otherwise} \end{cases},$$

where $\hat{D}_t^j = 1$ means the target j has been successfully detected at instant t . A χ^2 test is defined, consisting of computing the distance between the expected value and the obtained value of D_t^j . If the χ^2 test result suggests disappearance of the target j , as far as the collaborative MTT scheme is concerned, this reduction only leads to reduce the number of targets M and to remove the component j of maintained Gaussian distributions.

7. Simulation results

We evaluate and compare the performance of the proposed MTT scheme on a challenging synthetic tracking problem. The simulated WSN had 400 sensors, which were assumed to be uniformly deployed in a 2-dimensional field ($100 \times 100 \text{m}^2$), and their sensing ranges were identically fixed to 10m in order to ensure the three-coverage condition. The range-based observation model formulated in Equation (5) was adopted. The involved communication noise, defined by ϵ^j , was assumed to be identical and white Gaussian distributed, with covariance $\sigma_{\epsilon^j}^2 = 0.05$. After the deployment step, the network field is under the surveillance of all the sensors, in order to detect

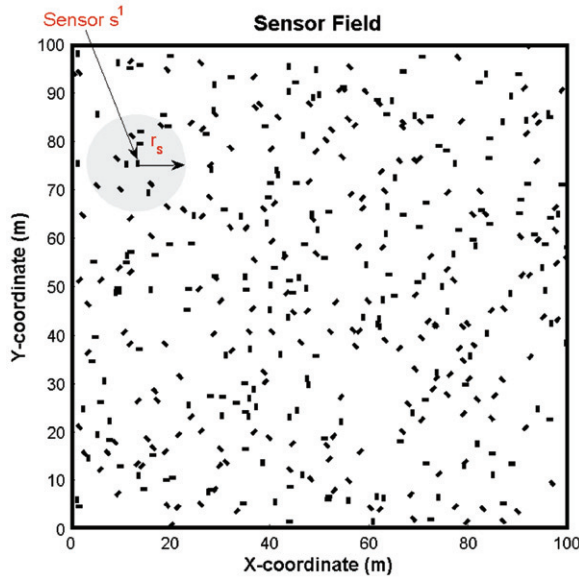


Figure 4. Demonstration of the initialisation state of the sensor field. Sensors are randomly and densely deployed in the surveillance field, denoted by the small black rectangles. The sensor of ID 1 is denoted by s^1 , and with the sensing range $r_s = 10$ m represented by a grey disk, which is identical to that of the other sensors.

any intrusion. The initial configuration of the WSN is illustrated in Figure 4.

To establish a baseline performance evaluation, the synthetic example is demonstrated by Figure 5, where the target trajectories are denoted by their coordinates in the sensor field. At instant $t=1$, two targets, denoted by a blue circle (target A), and a red diamond (target B) respectively, intrude into the surveillance field. The sensors that detect their appearances communicate with each other to form signal processing clusters. As the two targets are far apart till $t=40$, they are separately tracked by their corresponding sensor clusters, leading to a simple extension of single target tracking with the VF. At instant $t=40$, a new target denoted by a black star (target C) is detected in the WSN. In fact, the new target C is close to the old target B, leading to data association ambiguity. The method proposed in Section 6 is adopted to detect the appearance of the new target C. The SMCDA phase is thus invoked to assign the ambiguous observation data and to track the target B and C together with the VF algorithm. The target A is separately tracked by its corresponding cluster at that time. The three targets move closely between the instant $t=45$ and the instant $t=80$, and are thus tracked together by the collaborative MTT scheme using the SMC and

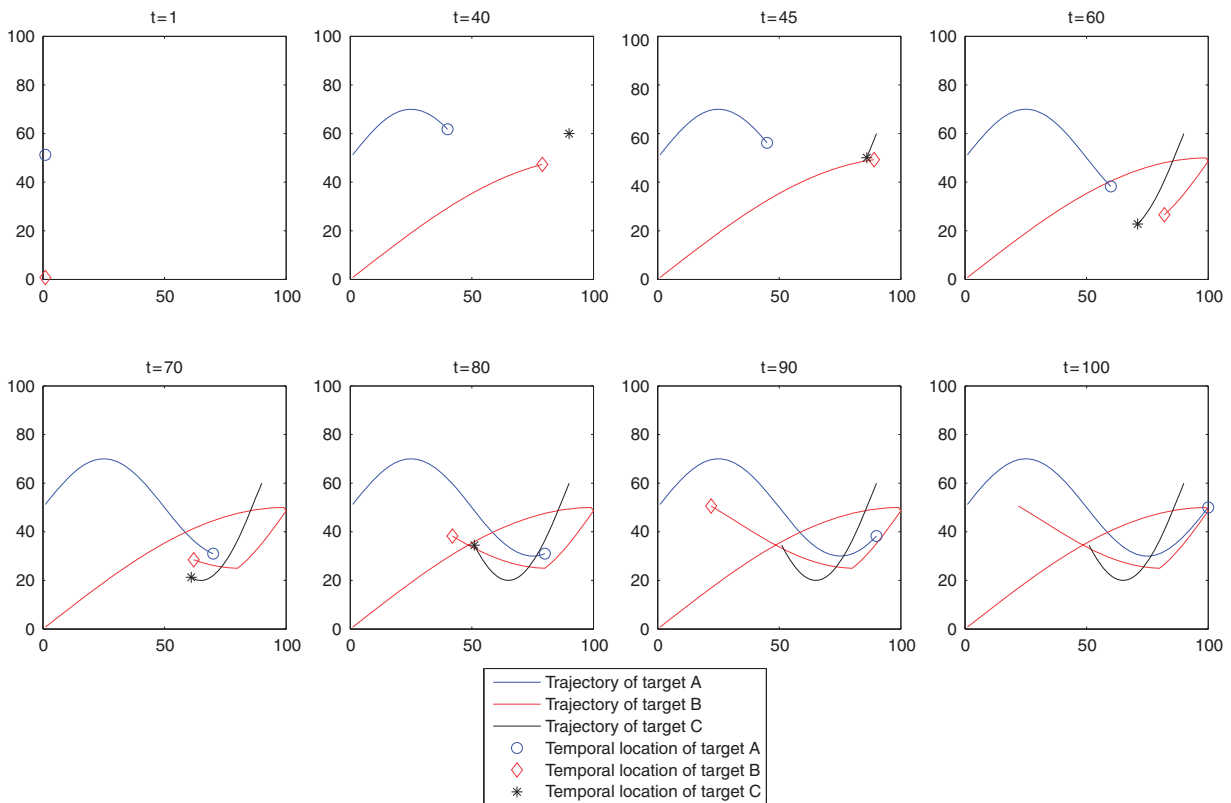


Figure 5. Synthetic multi-target tracking example.

the VF methods. At instant $t=80$, the target C disappears. At this time, all the three targets are close to each other. The hypothesis testing method is thus employed in the merging CH_t to detect the disappearance of target C. Whereas the disappearance of the target B is simply detected as the targets are scattered and tracked separately. From the instant $t=90$, no sensor in the network has detected the target B any more. Finally, the target A leaves the surveillance field at instant $t=100$. Therefore, all the exception cases are involved in the synthetic example to evaluate the proposed scheme.

Despite of distinct velocities and trajectories of the three targets, they are all described by the general state evolution model. The initial parameters are identically set for all the targets as follows:

$$\bar{\lambda}^j = \begin{bmatrix} 1/100 & 0 \\ 0 & 1/100 \end{bmatrix}, \quad \bar{V}^j = \begin{bmatrix} 10 & 0 \\ 0 & 10 \end{bmatrix}, \quad \bar{n}^j = 10, \\ \forall j = 1, \dots, M.$$

However, the initial value of the expectation μ_0^j is not identical for all the targets. It is initialised with the centroid of the sensors which have detected the target j . Owing to the flexibility of the general state evolution model, the target states are successfully tracked despite their distinct trajectory properties. The performance of the proposed scheme after one typical run is shown in Figure 6(a), where acceptable tracking performance is achieved. The corresponding root mean square error (RMSE) is shown in Figure 6(b), where one can note that the VF succeeds in tracking the targets in the separate case. When the new target C arrived at $t=40$,

the two targets B and C are close to each other (between $t=40$ and $t=50$) and the tracking performance degrades because of data association ambiguity. The tracking errors of target A remain quite low during the same period, as it is far from the other two targets and is separately tracked by its corresponding cluster of detecting sensors. However, the maximal estimation errors during the period between $t=40$ and $t=50$ of the target B is 1.4083 and that of the target C is 0.9164, which are still acceptable. During the period $t=64$ to $t=73$, all the three targets encounter each other. The data association becomes therefore more difficult, leading to worse tracking performance of the targets. The maximal estimation error for the target A is $\max(\text{Error}^A) = 1.8803$, for the target B is $\max(\text{Error}^B) = 3.1348$ and that of the target C is $\max(\text{Error}^C) = 1.5020$. As can be expected and shown in Figure 6(a), although the proposed collaborative MTT scheme succeeds in distinguishing the three targets, the tracking performance is not as good as that when the targets are tracked separately. If there is an ambiguity about the target state due to the clutter, or if the measurements come from multiple-target, multiple modes arise. Unfortunately, one important shortcoming of particle filters, in general, is that they yield poor results in maintaining the multi-modality of the target distribution. In a practical particle filter implementation, however, it often happens that all the particles quickly migrate to one of the modes, subsequently discarding all other modes. As a result, the estimates of the three targets converge towards a same mode, which is the centroid of their temporal positions.

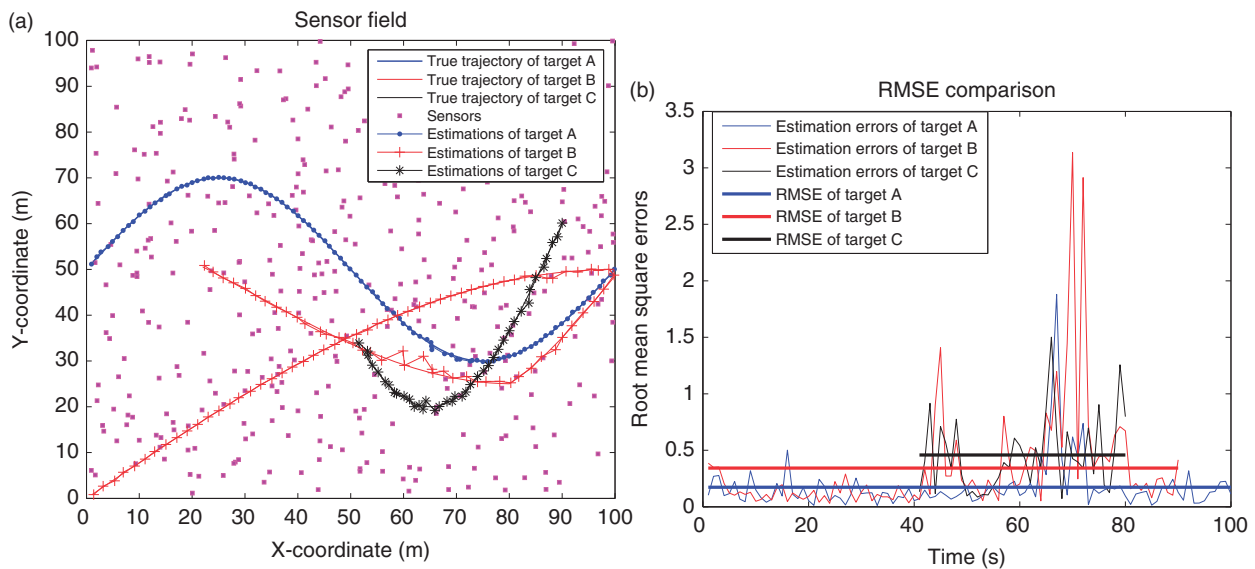


Figure 6. Multi-target tracking performance: (a) Multi-target tracking scenery and (b) Root Mean Square Error of MTT.

Table 1. Tracking accuracy of the collaborative MTT Scheme.

Evaluation	Target A	Target B	Target C
Average RMSE (m)	0.1743	0.6096	0.5455
Maximal estimate error (m)	1.8803	3.1348	1.5020

Table 2. Evaluation of the collaborative MTT Scheme.

Evaluation	
Overall energy consumption	CHs: 9.71 mJ Slaves: 3.21 mJ
Average energy consumption	100.67 μ J/CH 25.14 μ J/Slave
Execution time	0.2725 s

Monte Carlo simulations were performed on the same configuration, where $N = 200$ particles were used. The tracking results with respect to the targets are reported in Table 1. The tracking accuracy is evaluated by the average RMSE of the 100 runs of Monte Carlo simulations. To calculate the energy expenditure during the whole process, we adopt the following hypotheses:

- the intra-cluster communication and the inter-cluster communication between neighbouring CHs are via single hops;
- the energy consumed in computation can be neglected relative to energy consumed in communication.

According to the energy consumption model proposed in Chhetri, Morrell, and Suppappola (2005) and Wu and Abouzeid (2005), the energy consumed in transmission per bit is $E_T = \epsilon_e + \epsilon_a d^3$, where ϵ_e is the energy consumed by the circuit per bit, ϵ_a is the energy dissipated in *Joules* per bit per m^3 and d is the transmission distance ($\epsilon_a = 3.5 \times 10^{-3}$ pJ/bit/ m^3 , $\epsilon_e = 45$ nJ/bit). The energy consumed when receiving data is given by $E_R = \epsilon_r N$, where ϵ_r denotes the energy expended on receiving one bit of data ($\epsilon_r = 135$ nJ/bit). Similarly, the energy consumed in detection is defined by $E_S = \epsilon_s N$, where ϵ_s is the energy expended on sensing one bit of data ($\epsilon_s = 50$ nJ/bit). We calculate the overall and the average energy consumptions of the CHs and the slave sensors, respectively. Concerning the execution time, it is evaluated by the average time consumed per sampling slot (1 s). As shown in the Table 2, the average execution time of 0.2725 s guarantees the on-line implementation of our scheme.

To benchmark the performance of our collaborative MTT scheme against the classical SMC MTT algorithm, we adopt the identical synthetic scenery in Vermaak et al. (2005), which tracked three slowly manoeuvring targets in the 2-D plane. Each target were modelled with the near constant velocity model. The example trajectories for $M = 3$ targets are shown in Figure 7, where we run the algorithms with an increasing number of particles, i.e. $N = 100, 200, 400, 800$. As expected, the estimated trajectories of the proposed collaborative MTT scheme become more accurate as the difficulty of the MTT problem decreases compared with the synthetic example above. Due to the collision of the targets, both the algorithms were unable to disambiguate all the targets, leading to degraded tracking performances.

To get a statistical reflection of the behaviour of the algorithms, we run Monte Carlo simulations of each experiment for 20 times. As shown in the Table 3, the RMSE generally decreases with an increase in the number of particles. However, the performance does not appear to upgrade significantly. With respect to the RMSE of different targets, their estimated locations are of different accuracies in the classical SMC MTT algorithm, whereas similar tracking precisions are illustrated for the proposed collaborative MTT scheme. In fact, in the classical SMC MTT algorithm (Vermaak et al. 2005), only two sensors are used. Therefore, the target that is closer to the observer gets more accurate estimations. On the other hand, they do not consider the energy consumption in the two sensors. Furthermore, in addition to the range observation, bearing information is also need for the tracking, which thus necessitates additional hardware configuration. The computational complexity is reflected by the average execution time statistics in the Table 3. Both the algorithms exhibit the same trend, with the execution time increasing with the increase in the number of particles. Acceptable error performance are achieved while the average execution time per time step is well within the limits of practically reliable systems. However, due to the incorporation of much more numbers of measurements, our scheme is computationally more expensive, with better tracking performance.

8. Conclusion and perspectives

A distributed VF solution to multi-target tracking is proposed in the context of WSN. As the targets can travel arbitrarily and no *a priori* information on the targets motion is provided, a general state evolution model is proposed to describe the hidden state.

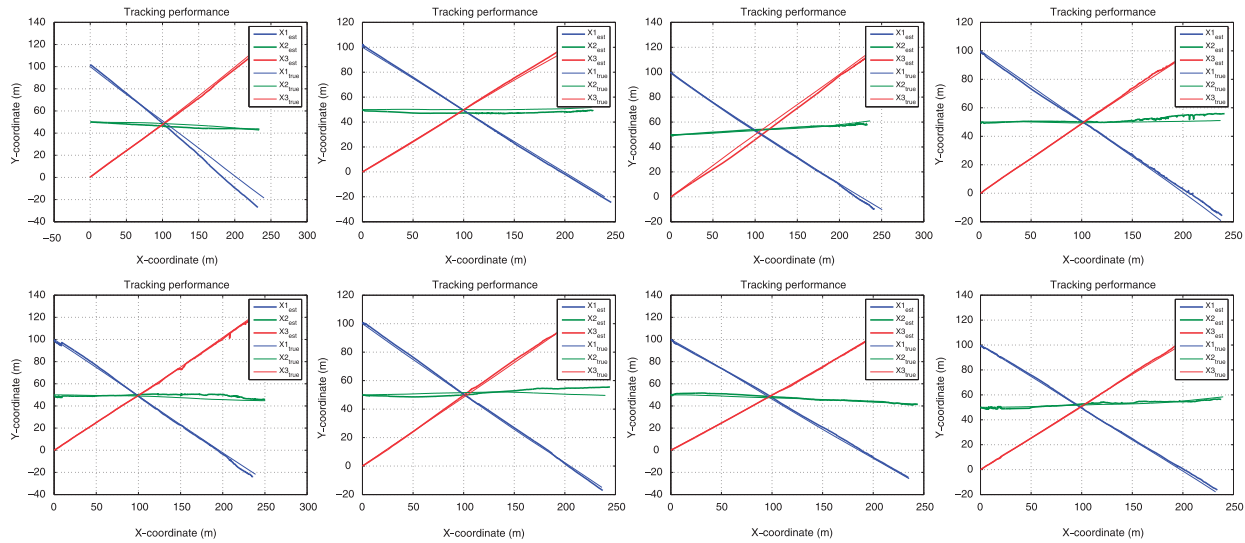


Figure 7. Example trajectories for three slowly manoeuvring targets. The columns from left to right illustrate the tracking performance using $N = 100, 200, 400, 800$, respectively. The top row is for the classical SMC MTT algorithm, and the bottom row for the proposed Collaborative MTT scheme.

Table 3. Comparison of the proposed MTT scheme against the classical SMC MTT algorithm.

Number of particles		100	200	400	800
Classical SMC MTT Algorithm	RMSE of tracking target x^1 (m)	1.0550	1.4701	1.2306	0.8725
	RMSE of tracking target x^2 (m)	2.4832	2.7389	2.3114	1.7833
	RMSE of tracking target x^3 (m)	5.2755	5.1364	4.0097	3.8661
	Execution time (s)	0.0116	0.0131	0.0184	0.0267
Proposed Collaborative MTT Scheme	RMSE of tracking target x^1 (m)	0.1326	0.1217	0.1305	0.0940
	RMSE of tracking target x^2 (m)	0.1044	0.1025	0.0965	0.0799
	RMSE of tracking target x^3 (m)	0.1252	0.1379	0.1038	0.0863
	Execution time (s)	0.2514	0.2720	0.3312	0.4187

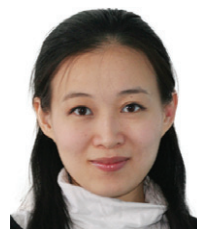
To minimise the resource consumption in WSN, an collaborative signal processing scheme is adopted. The MTT problem is reduced to single target tracking when targets are far apart, and probabilistic data association is invoked only when ambiguous observations are collected. In addition, the VF algorithm is executed on a fully distributed cluster base. Only the sensors which have detected the appearances of targets are activated to form a data processing cluster for energy efficiency. Furthermore, the variational method allows an implicit compression of the exchanged statistics between clusters. As shown in the simulations, estimates of the targets are continuously updated on-line even with data association ambiguity. Concerning the multi-modality problem arisen in the data association phase, we are thinking of integrating the method proposed in (Vermaak, Doucet, and Pérez 2003a) into the collaborative scheme, to maintain the

multi-modality property inherent to target tracking problems.

Acknowledgements

This work has been supported by CSC (China Scholarship Council) funding, CPERCapSec program of Champagne-Ardenne Region and OSEO Champagne Ardenne.

Notes on contributors



Jing Teng received her BEng degree in Electronic Information Engineering from the Central South University, China, in 2003, and her PhD degree in Systems Optimisation and Security from the University of Technology of Troyes, France, in 2009. Since 2010, she has been a lecturer at the North China Electric Power University. Her

research interests include statistical signal processing and its applications in wireless sensor networks. She has authored more than 10 papers in refereed journals and international conference proceedings, and has been serving as a reviewer of several journals and international conferences in these areas. She is a member of the IEEE and the IEEE Signal Processing Society.



Hichem Snoussi received a diploma in electrical engineering from the Ecole Supérieure d'Electricité (Supélec), Gif-sur-Yvette, France, in 2000, and the DEA and Ph.D. degrees in signal processing from the University of Paris-Sud, Orsay, France, in 2000 and 2003, respectively. He has obtained the HDR from the University of

Technology of Compiègne in 2009. Between 2003 and 2004, he was postdoctoral researcher at IRCCyN, Institut de Recherches en Communications et Cybernétiques de Nantes. He has spent short periods as visiting scientist at the Brain Science Institute, RIKEN, Japan and Olin Neuropsychiatry Research Center at the Institute of Living in USA. Between 2005 and 2010, he has been associate professor at the University of Technology of Troyes. Since September 2010, he has been appointed a Full Professor position at the same university. He is in charge of the regional research program S3 (System Security and Safety) of the CPER 2007–2013 and the CapSec platform (wireless embedded sensors for security). He is the principal investigator of an ANR-Blanc project (mv-EMD), a CRCA project and a GDR-ISIS young researcher project. He is partner of many ANR projects, GIS, strategic UTT programs. He obtained the national doctoral and research supervising award PEDR 2008–2012.



Cédric Richard received his Dipl.-Ing. and MS degrees, in 1994, and his PhD degree, in 1998, from the University of Technology of Compiègne, France, all in Electrical and Computer Engineering. From 1999 to 2003, he was an Associate Professor at the University of Technology of Troyes (UTT), France. From 2003 to 2009, he

was a Full Professor at the Institut Charles Delaunay (CNRS FRE 2848) at the UTT, and the supervisor of a group consisting of 60 researchers and PhDs. In winter 2009, he was a Visiting Researcher with the Department of Electrical Engineering, Federal University of Santa Catarina (UFSC), Florianópolis, Brazil. Since September 2009, Cédric Richard has been a Full Professor at Fizeau Laboratory (UNS, CNRS UMR 6525, Observatoire de la Côte d'Azur), University of Nice Sophia-Antipolis, France. His current research interests include statistical signal processing and machine learning. Prof Cédric Richard is the author of over 100 papers. He is a member of GRETSI association board and of the EURASIP society, and Senior Member of the IEEE. Cédric Richard serves as an Associate Editor of the IEEE Transactions on Signal Processing since 2006, and of the EURASIP Signal Processing Magazine since 2009.

References

- Bar-Shalom, Y., and Fortmann, T.E. (1988), *Tracking and Data Association*, San Diego, CA, USA: Academic Press Professional, Inc.
- Blackman, S.S., and Popoli, R. (1999), *Design and Analysis of Modern Tracking Systems*, Boston, London: Artech House Books.
- Chen, W., Hou, J.C., and Sha, L. (2004), 'Dynamic Clustering for Acoustic Target Tracking in Wireless Sensor Networks', *IEEE Transactions on Mobile Computing*, 3, 258–271.
- Chhetri, A.S., Morrell, D., and Suppappola, A.P. (2005), 'Energy Efficient Target Tracking in a Sensor Network Using Non-myopic Sensor Scheduling', in *The 7th International Conference on Information Fusion*, 25–29 July, Philadelphia, PA, USA, pp. 558–565.
- Djurić, P.M., Vemula, M., Bugallo, M., and Míguez, J. (2005), 'Non-cooperative Localization of Binary Sensors', in *Proceedings of the 13th Workshop on Statistical Signal Processing*, 17–20 July 2005, Bordeaux, France, pp. 1244–1249.
- Fortmann, T.E., Bar-Shalom, Y., and Scheffe, M. (1980), 'Multi-target Tracking using Joint Probabilistic Data Association', in *Proceedings of the 19th IEEE Conference on Decision and Control including the Symposium on Adaptive Processes*, 10–12 December, Albuquerque, New Mexico, pp. 807–812.
- He, G., and Hou, J.C. (2005), 'Tracking Targets with Quality in Wireless Sensor Networks', in *Proceedings of the 13th IEEE International Conference on Network Protocols*, 6–9 November, Boston, MA, USA, pp. 63–74.
- He, T., Huang, C., Blum, B.M., Stankovic, J.A., and Abdelzaher, T. (2003), 'Range-free Localization Schemes for Large Scale Sensor Networks', in *Proceedings of the 9th Annual International Conference on Mobile Computing and Networking*, 14–19 September, San Diego, California, USA, pp. 81–95.
- Hue, C., Le Cadre, J.P., and Pérez, P. (2002a), 'Sequential Monte Carlo Methods for Multiple Target Tracking and Data Fusion', *IEEE Transactions on Signal Processing*, 50, 309–325.
- Hue, C., Le Cadre, J.P., and Pérez, P. (2002b), 'Tracking Multiple Objects with Particle Filtering', *IEEE Transactions on Aerospace and Electronic Systems*, 38, 791–812.
- Hue, C., Le Cadre, J.P., and Pérez, P. (2006), 'Posterior Cramer-rAo Bounds for Multi-target Tracking', *IEEE Transactions on Aerospace and Electronic Systems*, 42, 37–49.
- Khan, Z., Balch, T., and Dellaert, F. (2006), 'McMC Data Association and Sparse Factorization Updating for Real Time Multitarget Tracking with Merged and Multiple Measurements', *IEEE Transactions on Pattern Analysis and Machine Intelligence*, 28, 1960–1972.
- Kreucher, C., Kastella, K., and Hero, A.O. (2005), 'Multitarget Tracking Using a Particle Filter Representation of the Joint Multitarget Density', *IEEE*

- Transactions on Aerospace and Electronic Systems*, 41, 1396–1414.
- Li, X.R., and Bar-Shalom, Y. (1996), ‘Tracking in Clutter with Nearest Neighbour Filters: Analysis and Performance’, *IEEE Transactions on Aerospace and Electronic Systems*, 32, 995–1010.
- Liu, J., Chu, M., and Reich, J.E. (2007), ‘Multi-target Tracking in Distributed Sensor Networks’, *IEEE Signal Processing Magazine*, 24, 36–46.
- Oh, S., Russell, S., and Sastry, S. (2004), ‘Markov Chain Monte Carlo Data Association for General Multiple-target Tracking Problems’, in *Proceedings of the 43rd IEEE Conference on Decision and Control*, 14–17 December, Atlantis, Paradise Island, Bahamas, pp. 735–742.
- Reid, D.B. (1979), ‘An Algorithm for Tracking Multiple Targets’, *IEEE Transactions on Automatic Control*, 24, 843–854.
- Snoussi, H., and Richard, C. (2006), ‘Ensemble Learning Online Filtering in Wireless Sensor Networks’, in *Proceedings of the 10th IEEE International Conference on Communications Systems*, 30 October–1 November, Singapore, pp. 1–5.
- Song, T.L., Lee, D.G., and Ryu, J. (2005), ‘A Probabilistic Nearest Neighbour Filter Algorithm for Tracking in a Clutter Environment’, *Signal Processing*, 85, 2044–2053.
- Song, X., Cui, J., Zha, H., and Zhao, H. (2008), ‘Vision-based Multiple Interacting Targets Tracking via On-line Supervised Learning’, in *Proceedings of European Conference on Computer Vision, ECCV’08*, pp. 642–655.
- Teng, J., Snoussi, H., and Richard, C. (2007a), ‘Binary Variational Filtering for Target Tracking in Sensor Networks’, in *Proceedings of the 2007 IEEE/SP 14th Workshop on Statistical Signal Processing*, 26–29 August, Madison, WI, USA, pp. 685–689.
- Teng, J., Snoussi, H., and Richard, C. (2007b), ‘Prediction-based Proactive Cluster Target Tracking Protocol for Binary Sensor Networks’, in *Proceedings of the 7th IEEE International Symposium on Signal Processing and Information Technology*, 15–18 December, Cairo, Egypt, pp. 234–239.
- Teng, J., Snoussi, H., and Richard, C. (2010), ‘Decentralised Variational Filtering for Target Tracking in Binary Sensor Networks’, *IEEE Transactions on Mobile Computing*, 9, 1465–1477.
- Teng, J., Snoussi, H., Richard, C., and Zhou, Y. (2009), ‘Hybrid Probabilistic Data Association and Variational Filtering for Multi-Target Tracking in Wireless Sensor Networks’, in *Proceedings of the 3rd International Workshop on Computational Advances in Multi-Sensor Adaptive Processing (CAMSAP 2009)*, 13–16 December, Aruba, Dutch Antilles, pp. 368–371.
- Vermaak, J., Doucet, A., and Pérez, P. (2003a), ‘Maintaining Multi-Modality Through Mixture Tracking’, in *Proceedings of the 9th IEEE International Conference on Computer Vision*, 14–17 October, Nice, France, pp. 1110–1116.
- Vermaak, J., Godsill, S.J., and Pérez, P. (2005), ‘Monte Carlo Filtering for Multi Target Tracking and Data Association’, *IEEE Transactions on Aerospace and Electronic Systems*, 41, 309–332.
- Vermaak, J., Lawrence, N.D., and Pérez, P. (2003b), ‘Variational Inference for Visual Tracking’, in *Proceedings of the 2003 IEEE Computer Society Conference on Computer Vision and Pattern Recognition*, 16–22 June, Madison, Wisconsin, USA, pp. 773–780.
- Wu, H., and Abouzeid, A.A. (2005), ‘Error Robust Image Transport in Wireless Sensor Networks’, in *The 5th Workshop on Applications and Services in Wireless Networks*, 29 June–1 July, Paris, France, pp. 1–9.
- Yang, H., and Sikdar, B. (2003), ‘A Protocol for Tracking Mobile Targets using Sensor Networks’, in *Proceedings of the 1st IEEE International Workshop on Sensor Network Protocols and Applications*, 11 May, Anchorage, Alaska, USA, pp. 71–81.